2 CME CREDITS

SUPPLEMENT TO
MAY 2007

APPLIED RADIOLOGY®

THE JOURNAL OF PRACTICAL MEDICAL IMAGING AND MANAGEMENT

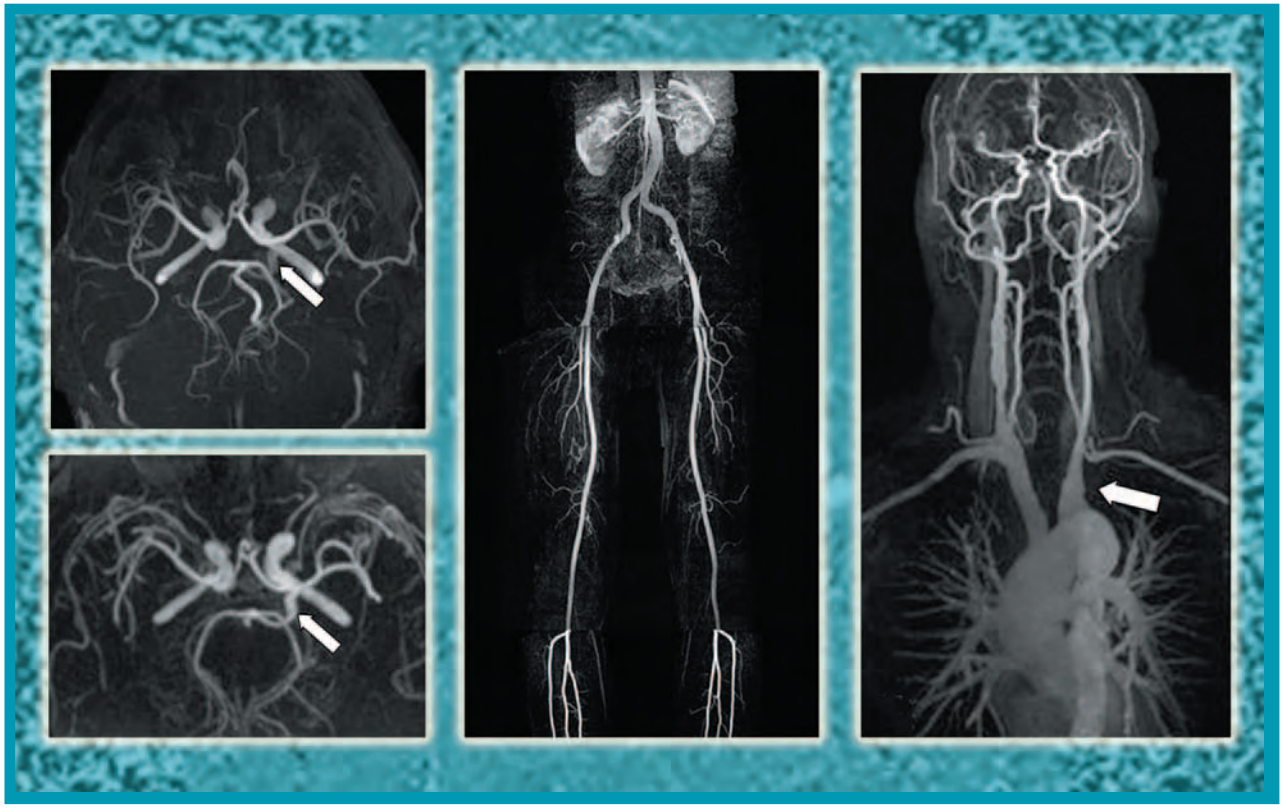

Contrast-Enhanced MRA Versus Nonenhanced MRA: Pros and Cons

Derek G. Lohan, MD; Roya Saleh, MD; Kambiz Nael, MD; Mayil Krishnam, MD; J. Paul Finn, MD

David Geffen School of Medicine at UCLA, Los Angeles, CA

Supported by an educational grant from

GE Healthcare

CME Category 1 Continuing Medical Education

This publication was supported by an educational grant from GE Healthcare, Princeton, NJ. The opinions expressed in this publication are those of the authors and not necessarily those of GE Healthcare or the editors or staff of *Applied Radiology*.

This activity has been planned and implemented in accordance with the Essential Areas and Policies of the Accreditation Council for Continuing Medical Education (ACCME) through the joint sponsorship of ArcMesa Educators and *Applied Radiology*. ArcMesa Educators is accredited by the ACCME to provide continuing medical education for physicians.

ArcMesa Educators designates this educational activity for a maximum of 2 AMA PRA Category 1 credits™. Physicians should only claim credit commensurate with the extent of their participation in the activity.

Target Audience

This activity is intended for radiologists.

Learning Objectives

At the conclusion of this program, the reader should be able to:

- Recognize the evolution of MRA to date, including practical details and the benefits and limitations of each technique.
- Recall the major current applications of these techniques in clinical practice.
- Identify the relative merits of each technique, with particular reference to the current and likely future roles of contrast-enhanced and non–contrast-enhanced MRA in diagnostic imaging.

Activity Description

Estimated time for completion: 2 hours
Date of release: May 1, 2007
Expiration date: May 1, 2008

This CME program consists of text and related images appearing in the article contained in this supplement and available online at www.appliedradiology.com/cme. You should read the article, review the accompanying images, refer to the references, and complete the self-evaluation quiz (available online at www.appliedradiology.com/cme or on page 16 of this publication) in order to be awarded CME credits. There is no charge for participating in this program.

Instructions for the online CME post test:

You must register with AR Online to access the online CME post test and to participate in the CME Accredited Activities:

1. Go to AR Online: www.appliedradiology.com
2. Register by clicking on "Register" in the top right corner.
3. Complete the registration form and click "Finish."
4. You will receive an email in order to authenticate your email address as your User ID.
5. Check your Inbox, Spam, or Junk Folder and open the email from AR Online.
6. The link in this message will take you to the AR Online login screen.
7. Once logged-in, click on "CME Activities" on the left navigation bar.
8. Select "MRI" programs.
9. Select the title of this program.
10. Once you have completed the activity, review the instructions, then click on the link to take the post test.
11. Upon successful completion, you will be able to print your certificate.

It is the policy of ArcMesa Educators to ensure balance, independence, objectivity, and scientific rigor in all its educational activities. All faculty/authors are expected to disclose any relevant financial relationships they may have with commercial interests in relation to this activity. These relationships, along with the educational content of this program, have been reviewed, and any potential conflicts of interest have been resolved to the satisfaction of ArcMesa Educators.

Dr. Lohan, Dr. Saleh, Dr. Nael, and Dr. Krishnam report that no such relationships exist. Dr. Finn reports relationships with GE Healthcare and Siemens Medical Solutions as a consultant.

Contrast-Enhanced MRA Versus Nonenhanced MRA

Publisher, *Applied Radiology*
O. Oliver Anderson

Associate Publisher, *Applied Radiology*
Kieran Anderson

Supplement Editor
Elizabeth A. McDonald

Supplement Assistant Editor
Beverly Harris

Supplement Editorial Assistant
Lisa M. Mangione

Art Director and Production
Barbara A. Shopiro

Contrast-enhanced MRA versus nonenhanced MRA: Pros and cons

Derek G. Lohan, MD; Roya Saleh, MD; Kambiz Nael, MD; Mayil Krishnam, MD; J. Paul Finn, MD

Abstract

Magnetic resonance angiography (MRA) continues to evolve rapidly, having grown from a variety of flow-dependent techniques through contrast-enhanced techniques, each with its own specific advantages and requirements. Recent technical developments such as the introduction of 3T scanners, the increasing sophistication of radiofrequency (RF) architecture, and the dissemination of parallel acquisition techniques have greatly increased the power and practicality of contrast-enhanced MRA, such that it is now highly competitive with computed tomographic angiography (CTA) in most vascular territories. Nonetheless, non–contrast-enhanced MRA is still widely used, particularly in neurovascular imaging. As a result, it is crucial that interpreting physicians are familiar with the basic principles, relative advantages, and limitations of each of these methods, including associated potential diagnostic pitfalls. The authors present the progression of nonenhanced and enhanced MRA to date, illustrating key characteristics as well as discussing the current applications of each in diagnostic imaging.

Conventional catheter angiography (CCA) has long been regarded as the gold standard for anatomic vascular imaging. However, CCA is invasive and expensive and exposes the patient to radiation and iodinated contrast agents.

Magnetic resonance angiography (MRA) has long held promise as an effective noninvasive alternative to CCA for many vascular territories. Early attempts at vessel analysis made use of time-of-flight (TOF) and phase-contrast (PC) techniques, while more recently contrast-enhanced (CE) MRA has gained wide acceptance, in many cases relegating conventional angiography to a secondary role during image-guided vascular intervention.

Dr. Lohan *is a Diagnostic Cardiovascular Imaging Fellow,* ***Dr. Saleh*** *is a Research Fellow,* ***Dr. Nael*** *is a Radiology Resident,* ***Dr. Krishnam*** *is an Assistant Professor of Radiology, and* ***Dr. Finn*** *is a Professor of Radiology and Medicine, Chief of Diagnostic Cardiovascular Imaging, and Director of Magnetic Resonance Research, Department of Radiology, David Geffen School of Medicine at UCLA, Los Angeles, CA.*

In this article, we discuss the evolving roles of CE-MRA relative to non–CE-MRA in clinical practice, drawing on our own experience and that of many others. We emphasize that there is a wide spectrum of hardware and software platforms on which MRA techniques are implemented and that the performance, quality, and reliability of the results are influenced by local platform configuration and operator skill.

Time-of-flight MRA

Time-of-flight (TOF) MRA takes advantage of through-plane blood flow to highlight patent blood vessels against a relatively suppressed stationary background.[1-3] Thus, the requirement for intravenous contrast administration is obviated. Furthermore, presaturation can be used effectively to eliminate signal (flow enhancement) from a specific direction, generating selective arteriograms or venograms in the brain and body.[4,5]

Time-of-flight MRA can be implemented in a 2-dimensional (2D) (sequential multislice) or a 3-dimensional (3D) (volume slab) format, depending on the target vascular territory. For the evaluation of detailed arterial anatomy, the 3D version is preferred, because it allows for isotropic voxels (by virtue of very thin digital slices, known as *partitions*). Three-dimensional TOF-MRA is time-consuming, taking approximately 5 to 10 minutes, depending on coverage and desired spatial resolution. For this reason, its applications are limited to structures such as the head and neck, which can be immobilized during the acquisition. Because of the widespread acceptance of neurovascular MR imaging (MRI), 3D TOF-MRA of the intracranial arteries is the single most widely used MRA technique of any kind. It is also commonly used for imaging the cervical carotid arteries.

The dependence on adequate flow enhancement imposes certain constraints on TOF-MRA. If the repetition time (TR) is too short, there will be insufficient time for fresh spins to enter the slice and vascular contrast will suffer. Also, if a vessel is oriented largely within the imaging slab or slice, the blood may become saturated (an effect known as in-plane saturation) even if flow is not severely

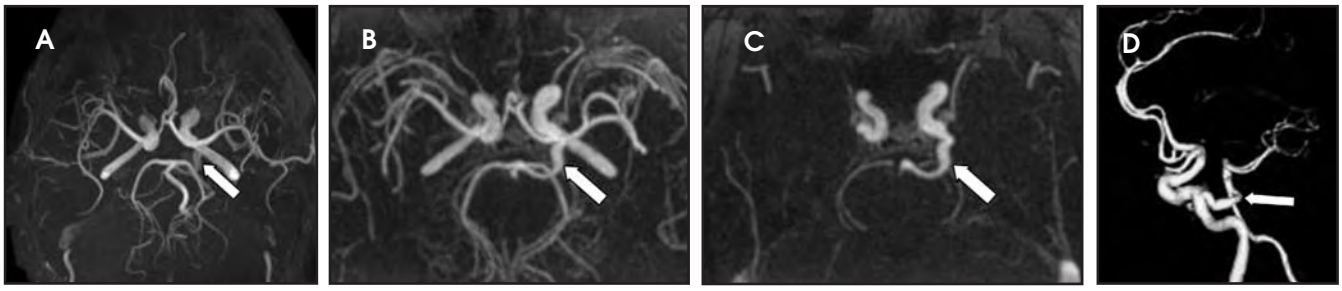

FIGURE 1. *Persistent left-sided trigeminal artery (arrows) as seen on (A) 3-dimensional (3D) time-of-flight MR angiography (MRA), (B) 3D contrast-enhanced (CE) MRA, (C) thin maximum intensity pixel reconstruction from 3D CE-MRA, and (D) sagittal volume-rendered projection derived from 3D CE-MRA data. This anomalous vessel is significantly more conspicuous on the contrast-enhanced images because of freedom from spin saturation, as seen in A. Contrast-enhanced MRA was performed with 14 mL of gadolinium.*

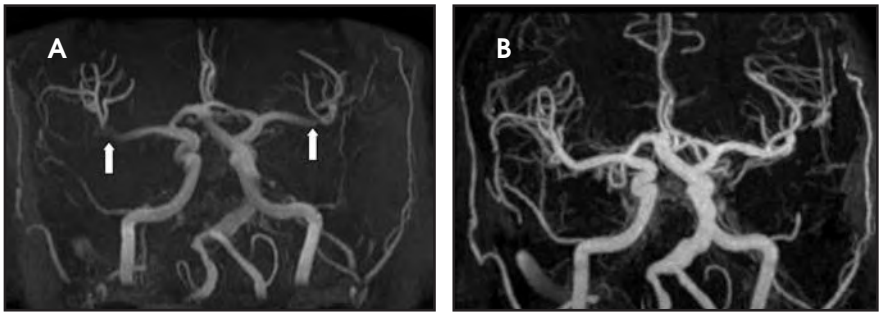

FIGURE 2. *(A) This in-plane 3-dimensional (3D) time-of-flight MR angiogram shows spin saturation (arrows) in the horizontal portions of the middle cerebral arteries bilaterally. (B) The corresponding magnified image from a 3D contrast-enhanced MR angiogram, during which data from the upper mediastinum to the vertex was obtained, shows freedom from such spin saturation.*

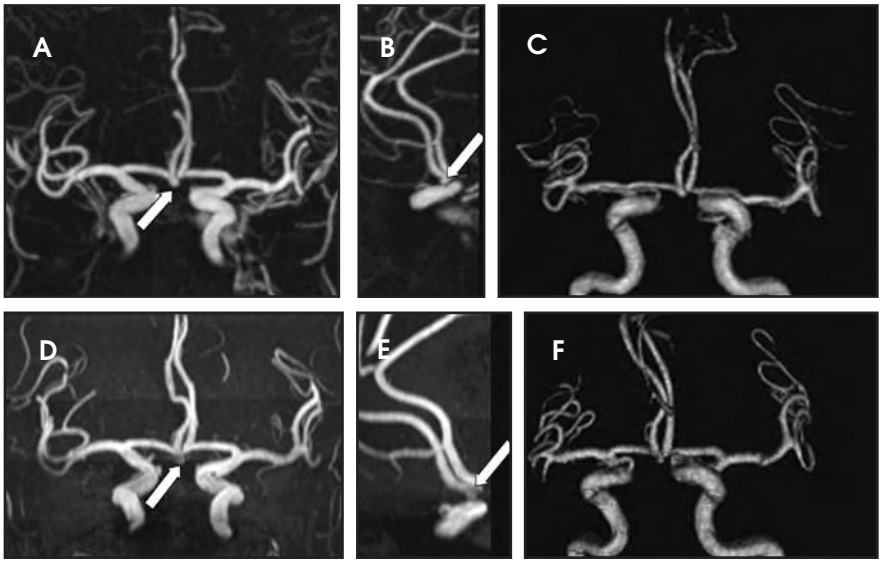

FIGURE 3. *Coronal and sagittal oblique maximum intensity projections (MIP) and 3-dimensional volume-rendered projections from (A, B, and C) contrast-enhanced MR angiography (MRA) and (D, E, and F) time-of-flight MR angiograms show a small inferiorly projecting saccular aneurysm (arrows) in the anterior communicating artery with a maximal diameter measurement of 2.6 x 3.1 mm. (Reprinted with permission from Nael K, Villablanca JP, Saleh R, et al. Contrast-enhanced MR angiography at 3T in the evaluation of intracranial aneurysms: A comparison with time-of-flight MR angiography.* AJNR Am J Neuroradiol. *2006;27:2118-2121.[6])*

compromised (Figures 1 through 9). For this reason, TR is generally chosen to balance acquisition time and flow enhancement. For TOF-MRA, TRs of approximately 20 to 40 msec are typical. Also, for a given TR, the flip angle is chosen in the range of 20˚ to 40˚ to optimize the blood signal while suppressing background. It was recognized early in the development of TOF-MRA that loss of signal within blood vessels can occur because of flow-induced phase dispersion, mimicking or exaggerating stenoses. This effect is more pronounced at longer echo times (TE), and it can be partially reversed by a technique known as gradient motion rephrasing.[2]

Outside the head and neck, breathing motion artifact generally renders 3D TOF-MRA useless. For this reason, TOF-MRA of the chest, abdomen, and pelvis has generally been implemented as a 2D, sequential breath-hold technique.[9-11] Two-dimensional TOF-MRA differs from its 3D counterpart in several important ways. With 3D TOF-MRA, the entire imaged volume is exposed to all the radiofrequency (RF) pulses, so that some degree of saturation is common and slowly flowing spins are poorly visualized. With 2D TOF-MRA, only a single slice is excited, so that through-plane flow sensitivity is heightened, and 2D TOF-MRA has been used to good effect for venous imaging,[12-14] where flow sensitivity is more important than spatial resolution. Slice thickness with 2D TOF-MRA is generally greater than partition thickness in 3D TOF-MRA. The acquisition order of the slices is sequential, such that each slice is independent of the others. For this reason, each slice can be acquired in an independent breath-hold, a useful property for abdominal and thoracic imaging. It should be pointed out that sequential 2D TOF-MRA is also commonly performed for the extracranial carotid arteries.[15,16]

Multiple overlapping thin-slab acquisition (MOTSA) MRA[17] represents a hybrid between sequential 2D MRA and single-slab 3D MRA. As the name suggests, with MOTSA, the thickness of each 3D slab is decreased in order to decrease saturation effects. Each overlapping subvolume is acquired sequentially and is finally fused with the others to form the complete 3D volume. Multiple overlapping thin-slab MRA is widely employed for imaging both the intracranial arteries and the extracranial carotids.[18,19]

The vulnerability of the blood to saturation during short TR 3D acquisition can be completely offset by the T1-shortening effect of paramagnetic contrast agents, as described in the early work of Prince et al[20] and Maki et al.[21] When the center of k-space is made to coincide with the peak intravascular concentration of a contrast bolus, the increase in blood signal is maximized. In recent years, developments in CE-MRA have benefited from steady improvements in RF architecture, gradient technology, parallel acquisition,[22-26] and the proliferation of 3T whole-body MR systems.[27-32]

Clinical applications

Three-dimensional TOF-MRA has long been the technique of choice for noninvasive imaging of the head and neck arteries.[33-37] For several reasons, the carotid circulation represents the most receptive anatomic region for 3D TOF-MRA. On average, the carotids have a predominantly superoinferior orientation and moderately high flow rates, making axial multislab acquisition suitable in most cases. It is practical to ask patients to keep their heads still for the several minutes required for a high-resolution study. Also, dedicated arrays of head-neck surface coils are widely available to maximize the signal-to-noise ratio (SNR) and to support parallel acquisition.

Indeed, when using an optimized technique on a cooperative patient, TOF-MRA allows superb visualization of the circle of Willis, which provides information about vascular patency, caliber, and the presence and location of intracranial aneurysms. This technique has shown particular value in the diagnosis, localization, and follow-up of patients with moyamoya disease and other intracranial vasculopathies. The majority of protocols use a MOTSA TOF technique to avoid the saturation effects of 3D TOF and to facilitate peripheral vessel depiction. However, knowledge of the limitations of TOF-MRA is important so that artifactual

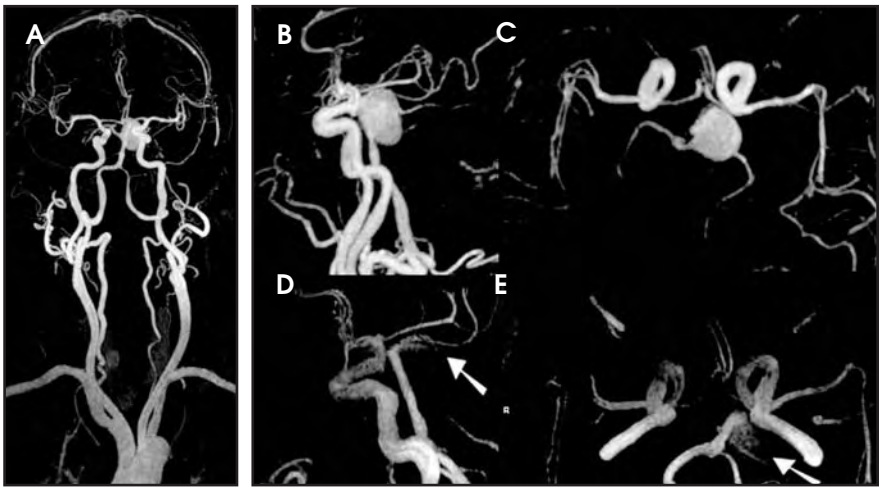

FIGURE 4. *(A) Coronal maximum intensity projection (MIP) from contrast-enhanced MR angiography (MRA) shows the supra-aortic arteries with voxel dimensions of 0.7 x 0.6 x 0.8 mm during 20 seconds. (B) Sagittal and (C) axial MIPs from contrast-enhanced MRA and (D and E) time-of-flight (TOF)-MRA show a 20 x 16-mm aneurysm arising from the basilar artery tip. The only portion of the aneurysm sac that is visualized on the TOF-MRA study is the superior portion (inflow zone) of the dome (arrows). The loss of signal intensity and incomplete enhancement of the aneurysm sac at TOF-MRA make the full sac size and geometry difficult to perceive. (Reprinted with permission from Nael K, Villablanca JP, Saleh R, et al. Contrast-enhanced MR angiography at 3T in the evaluation of intracranial aneurysms: A comparison with time-of-flight MR angiography.* AJNR Am J Neuroradiol. *2006;27:2118-2121.[6])*

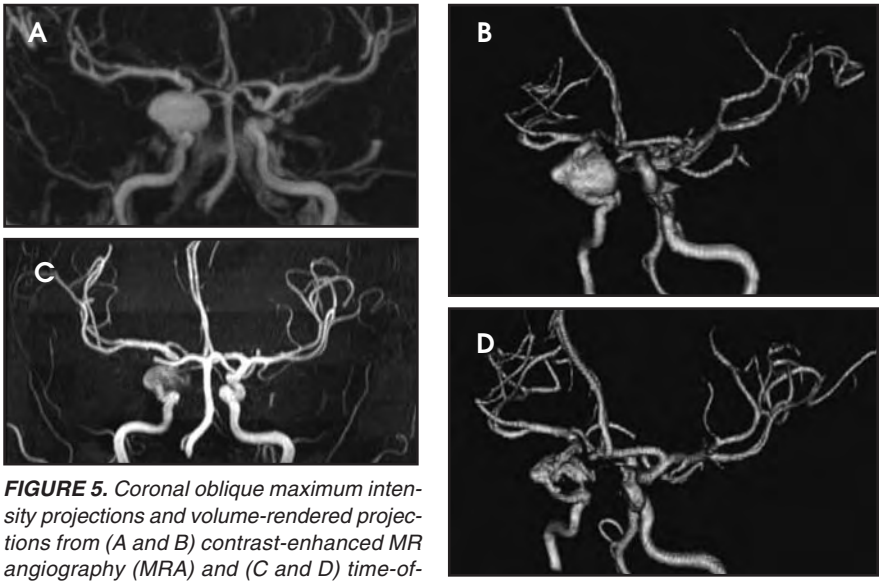

FIGURE 5. *Coronal oblique maximum intensity projections and volume-rendered projections from (A and B) contrast-enhanced MR angiography (MRA) and (C and D) time-of-flight (TOF) MRA show a large (16 x 12-mm) aneurysm arising from the cavernous portion of the right internal carotid artery. (C and D) At TOF-MRA, the loss of signal intensity and incomplete flow-related enhancement of the aneurysm sac limit definition of the border of the aneurysm. (Reprinted with permission from Nael K, Villablanca JP, Saleh R, et al. Contrast-enhanced MR angiography at 3T in the evaluation of intracranial aneurysms: A comparison with time-of-flight MR angiography.* AJNR Am J Neuroradiol. *2006;27:2118-2121.[6])*

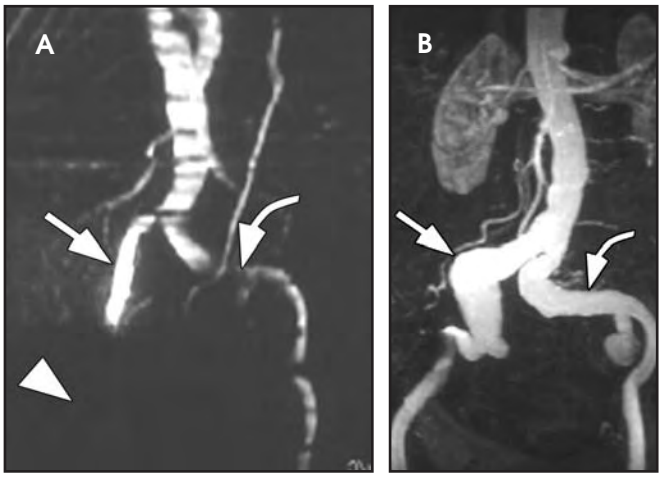

FIGURE 6. *(A) Two-dimensional time-of-flight (TOF) MR angiography (MRA) and (B) 3-dimensional (3D) contrast-enhanced (CE) MRA in the same patient show the advantages of 3D CE-MRA, which 1) eliminates slice misregistration and pulsatility artifacts, 2) reduces signal dropout from a right metallic hip (arrowhead), 3) more completely depicts slow flow in aneurysms (straight arrows), 4) reduces in-plane saturation artifact (curved arrows), and 5) shows a left internal iliac artery aneurysm. (Image courtesy of Thomas M. Grist, University of Wisconsin-Madison, WI and Martin R. Prince, Cornell University, NY; reprinted with permission from Prince MR, Grist TM, Debatin JF.* 3D Contrast MR Angiography*, 3rd ed. New York, NY: Springer Verlag; 2003:5.[7])*

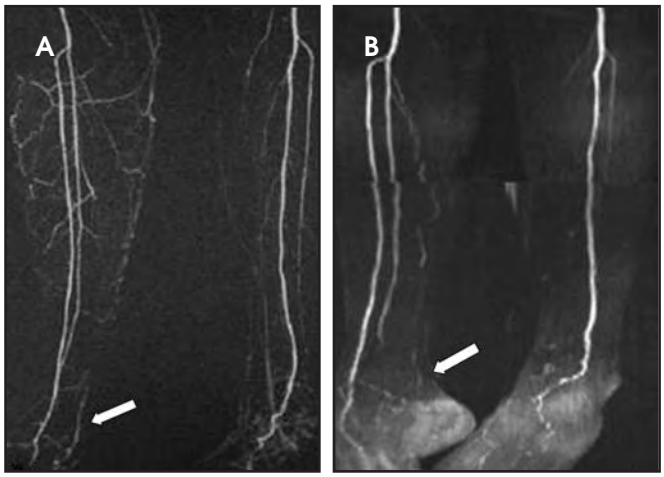

FIGURE 7. *(A) Hyper–time-resolved imaging of contrast kinetics, performed at 1.5T, shows a short segment of reconstituted posterior tibial artery at the right ankle. (B) The corresponding 2-dimensional (2D) time-of-flight (TOF) image fails to clearly depict this patent segment of the posterior tibial artery. The poor suppression of the soft tissues in the 2D TOF study leads to decreased vessel conspicuity. (Reprinted with permission from Thornton FJ, Du J, Suleiman SA, et al. High-resolution, time-resolved MRA provides superior definition of lower-extremity arterial segments compared to 2D time-of-flight imaging.* J Magn Reson Imaging. *2006;24:362-370.[8])*

stenoses and occlusions are recognized. Particularly in the region of the skull base and sphenoid sinus, susceptibility artifact due to bone and air may cause artifactual signal loss in the adjacent internal carotid artery. Intravoxel dephasing due to disturbed flow through the carotid siphon may also simulate stenosis, with a further reduction in the specificity of this technique if unrecognized. The importance of a complete data review, particularly of the source data images, has been repeatedly stressed in the literature,[38] so that these artifacts are not misinterpreted.

Recently, hardware technology has evolved to the point at which image quality with CE-MRA may rival or exceed that of TOF-MRA in the supra-aortic circulation. Several studies have addressed the usefulness of CE-MRA at 1.5T in the carotid[39] and vertebrobasilar circulations.[40] The increased SNR and gadolinium (Gd) sensitivity at 3T can be used to support aggressive parallel acquisition strategies during the first passage of a Gd bolus, resulting in even higher spatial resolution.[29,32] It could be argued that, with advanced machine hardware, CE-MRA may supersede TOF-MRA for most applications in the head and neck.

Phase-contrast MRA

Phase-contrast MRA (PC-MRA) involves the application of bipolar phase-encoding gradient pairs, to encode velocity in the direction of the gradient.[41] As a result, spins moving along the direction of the gradient field undergo a phase shift proportional to their velocity. Conversely, stationary tissue accumulates zero net phase (ideally). Subtraction of these flow-sensitive data sets from reference images allows visual representation of vascular flow and, thus, angiographic depiction. Importantly, as the phase shift experienced is proportional to the velocity of moving spins, phase-contrast imaging allows quantitative assessment of flow velocities (phase-contrast flow quantification—Figure 10).

Phase can have values only between +180˚ and –180˚. Typically, one half of the phase spectrum is assigned to flow in one direction and the other half to flow in the opposite direction. The flow sensitivity is determined by the gradient settings and is expressed by the velocity encoding value (Venc). The Venc is defined as the flow velocity that will result in a phase shift of 180˚. Ideally, the Venc is set for exactly the highest velocity flow expected in the vessel of interest. For slow flow, the Venc is set lower (eg, the portal vein may be 30 cm/sec), whereas for faster flow the Venc is set higher (eg, the aorta or just distal to a stenosis may be >200 cm/sec).

If the Venc chosen is too low, then velocity aliasing (wraparound) will occur, whereas if the Venc chosen is too high, the vascular contrast-to-noise ratio (CNR) will be low. Given that the greatest difference achievable between the flow-compensated and flow-sensitive data sets acquired during application of the bipolar gradient pairs occurs in opposite directions (ie, 180˚), phase shifts greater than the preselected Venc factor will be misrepresented in the image obtained. Therefore, this parameter must be carefully chosen so that artifactual reductions in signal intensity are not experienced, using higher Venc factors (>100 cm/sec) for regions of rapid arterial flow and lower Venc factors (20 to 30 cm/sec) for venous applications.[42]

Although PC-MRA can be made less vulnerable to saturation than TOF-MRA by choosing a small flip angle, there is still some T1 dependence, and the overall CNR can be increased by contrast injection. Gadolinium injection also makes it possible to use very short TRs, which decreases the acquisition time.

As is the case with TOF-MRA, PC-MRA may be applied as either a 2D projectional technique or a 3D technique. However, this latter volumetric technique is a time-consuming process, often requiring >20 minutes for image acquisition. Furthermore, PC-MRA is vulnerable to intravoxel dephasing, as is TOF-MRA. However, PC-MRA has the advantage of allowing interrogation of flow direction and improved visualization of slow-flow vessels even in regions with complex flow patterns.

Clinical applications

The potential application of PC-MRA to a variety of vascular territories has been evaluated, with generally satisfactory results.[43-45] The strength of this method lies in its ability to depict directional flow, as well as allowing quantitative analysis of flow characteristics. This is of particular value in the assessment of arteriovenous malformations, for which data acquisition using carefully selected Venc factors provide both arterial- and venous-phase images on sequential measurements with different Venc values. With the recent development of rapid high-resolution volumetric contrast-enhanced MRA techniques, however, PC-MRA is often reserved for research and "problem-solving" applications (Figures 11 through 13).

Steady-state free-precession MRA

Steady-state free precession (SSFP) exploits the coherent magnetization recoverable when TR <<T2. Steady-state free-precession MRA may generate rapid, bright-blood images without the requirement for Gd administration. With this technique, the images are not dependent on flow to generate vascular contrast, which is reflected more in the T2/T1 ratio of the blood. Also, SSFP techniques operate at very short TR (~3 msec) and large flip angles, generating bright-blood 2D images in <1 second. For this reason, breath-holding is not required for single-shot SSFP, and it may be used effectively for the evaluation of abdominal veins and the abdominal aorta. For the evaluation of the thoracic aorta (eg, to rule out dissection or aneurysm), electrocardiographic (EKG)-gated "segmented" SSFP cine has become a cornerstone technique.[47] Cine images can be acquired in a few seconds, and serious disease of the aorta can be ruled out or confirmed in as little as a few minutes.[48] Three-dimensional implementations of SSFP have been used successfully for imaging the coronary arteries, both in breath-hold[49] and free-breathing formats.[50] When combined with navigator-gating, free-breathing nonenhanced MRA in regions such as the chest becomes clinically feasible. However, SSFP-MRA is sensitive to off-resonance artifacts, which manifest as dark bands and ghosts that can be exacerbated by flow and motion. Off-resonance artifacts are more troublesome at higher field strengths, though a number of approaches have been described that address this challenging problem.[51]

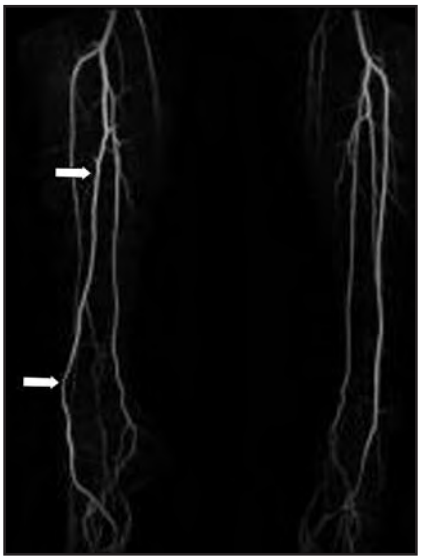

FIGURE 8. *Calf station from a peripheral contrast-enhanced MR angiographic study, which was performed at 3T. The arrows indicate the right peroneal artery, which is seen to continue across the ankle joint as the dorsalis pedis artery. This study was performed as a preoperative measure prior to fibular free flap creation; the above finding precluded the use of the right side for fibular resection.*

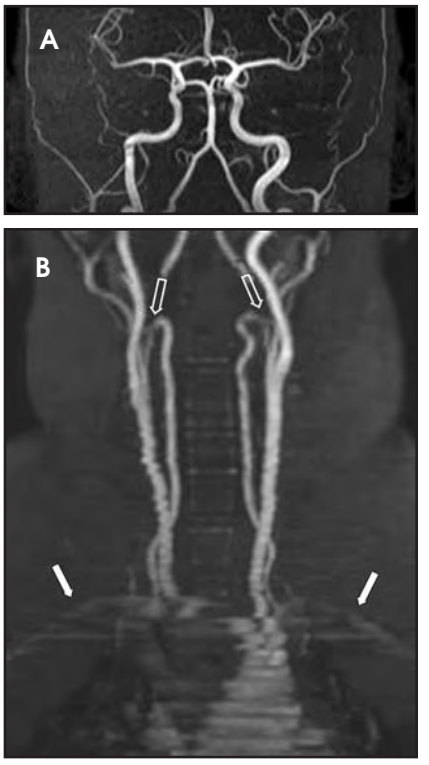

FIGURE 9. *Three-dimensional multiple overlapping thin-slab time-of-flight MR angiography of the (A) intracranial and (B) extracranial caroticovertebral circulation in the same patient. The absence of motion artifact makes this technique of high diagnostic value in the depiction of the intracranial vasculature. However, the presence of motion artifact (eg, swallowing) results in misregistration artifact with "stair-stepping" of the common carotid and vertebral arteries in the neck. Also noted is the presence of in-plane (ie, transverse) spin saturation with signal loss affecting the subclavian arteries (arrows) and horizontal portions of the vertebral arteries (open arrows) bilaterally.*

Clinical applications

As mentioned above, EKG-gated 3D SSFP-MRA has shown promise for coronary artery imaging, and CE-MRA of the coronary artery is challenging because of the conflicting requirements of first pass, rapid acquisition, and volume coverage.[49,51,52] Moreover, free-breathing angiography has performed well in a number of clinical scenarios, including aortic,[53] renal,[54] carotid,[55] and peripheral arterial imaging[56] (Figures 14 through 16).

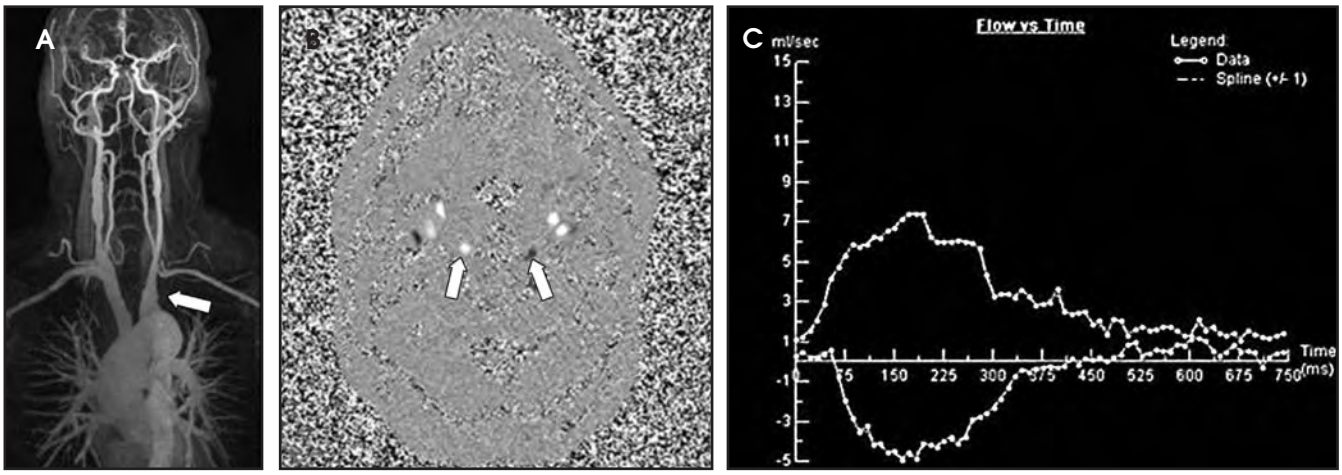

FIGURE 10. *Subclavian steal in a patient with Takayasu's arteritis. (A) A full-thickness maximum-intensity projection image derived from contrast-enhanced (CE) MR angiography (MRA), (B) a phase-contrast flow quantification, and (C) a temporal flow curve thus derived illustrate the presence of an occluded proximal left subclavian artery (arrow in A). However, CE-MRA does not allow quantitative assessment of left vertebral flow. (B and C) These images confirm the presence of opposite directional flow within the right and left vertebral arteries.*

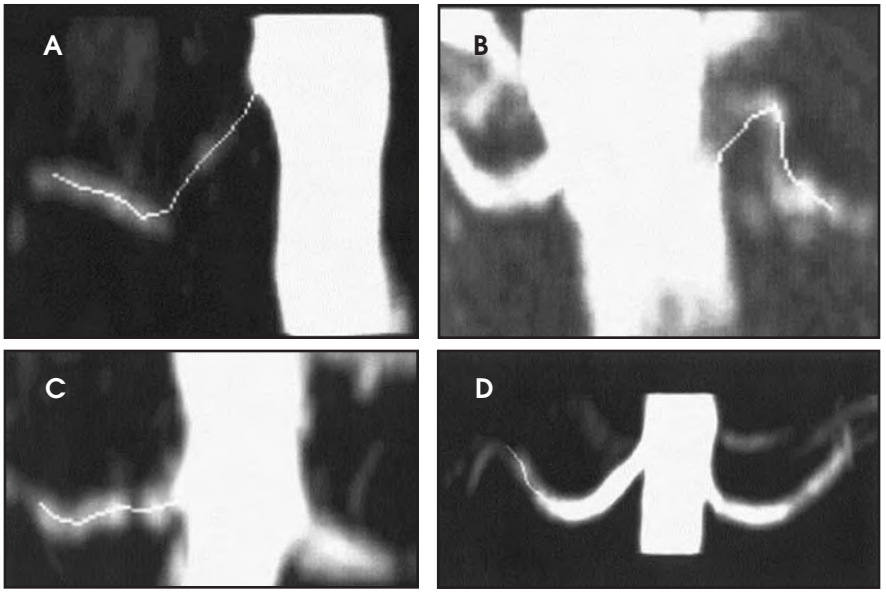

FIGURE 11. *(A, B, and C) Three-dimensional phase-contrast MR angiograms in 3 patients with varying degrees of renal artery stenosis. (D) A comparative normal study. (Images reprinted with permission from Westenberg JJ, van der Geest RJ, Wasser MN, et al. Objective stenosis quantification from poststenotic signal loss in phase-contrast magnetic resonance angiographic data sets of flow phantoms and renal arteries.* Magn Reson Imaging. *1998; 16:249-260.[46])*

FIGURE 12. *An axial 3-dimensional phase-contrast MR angiogram of the renal arteries in a normal subject. (Image courtesy of Martin R. Prince, Cornell University, New York, NY [www.mrprotocols.com].)*

Contrast-enhanced MRA (CE-MRA)

Contrast-enhanced MRA has become one of the most powerful and useful applications of MRI in recent years. It involves the intravenous administration of a bolus of a Gd-based T1-shortening contrast agent, which dramatically increases the signal intensity of blood on the first pass.[57] The blood signal greatly exceeds that of nonvascular background tissue on 3D T1-weighted ultrafast gradient-echo pulse sequences, such that high CNR angiograms are generated.

Contrast-enhanced MRA is based on the presence of Gd in the blood, independent of the flow waveform and flow velocity in the vessels. It does not rely upon the physiologic flow of in-phase spins for signal generation and is free from many of the limitations of TOF-MRA and PC-MRA that were considered above.[6] The basic pulse sequence for CE-MRA is an ultra-short TR/TE 3D spoiled gradient-echo sequence and has a relatively simple structure. The TR is made as short as possible to speed up image acquisition and capture the first pass of contrast. The presence of Gd makes the blood immune to saturation, so the short TR tends to saturate only background tissue. In general, the highest flip angle achievable by the MRI machine is used, which is consistent with RF-specific absorption rate (SAR) limits that are mandated by the Food and Drug Administration. The TE is also made as short as possible—ideally approximately 1.0 msec, so as to limit any flow-induced dephasing effects. For this reason, vessel diameters measured on high-quality CE-MRA studies tend to have far less exaggeration of stenosis due to turbulent flow. Several examples are shown below.

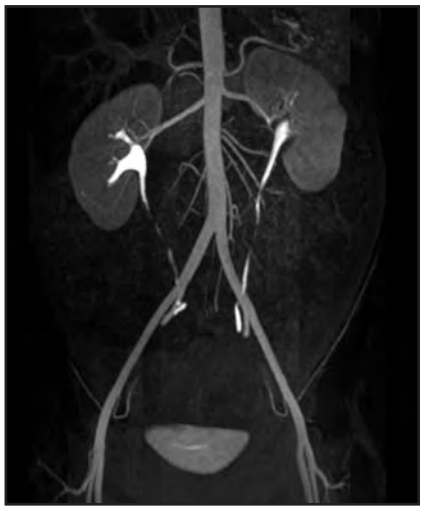

FIGURE 13. *A comparative full-thickness maximum-intensity projection reconstruction of 3-dimensional contrast-enhanced MR angiographic examination of the renal arteries, which allows confident exclusion of renal artery stenosis. The extended field of view that this image provides facilitates the exclusion of vascular pathology within the entire abdomen and pelvis.*

However, CE-MRA is highly dependent on accurate timing of the contrast bolus. Attention must be paid to the following factors:

1) Coordinating image acquisition with the arrival of the contrast bolus within the vessels of interest;
2) Filling the center of k-space during the peak period of contrast enhancement;
3) Using the smallest Gd dosage possible that will produce diagnostic image quality;
4) Obtaining high-resolution arterial data acquisition while minimizing detrimental venous enhancement; and
5) Preventing patient motion during acquisition, particularly respiratory motion during chest and abdominal imaging.

A number of methods are used to time the bolus, including the use of a fixed timing delay, a test bolus, repeated multiphase scanning, and real-time fluoroscopic detection of contrast arrival.[58] Our experience has been that the injection of a small test bolus yields the most consistent results, confirms the integrity of the intravenous access site, and facilitates planning.

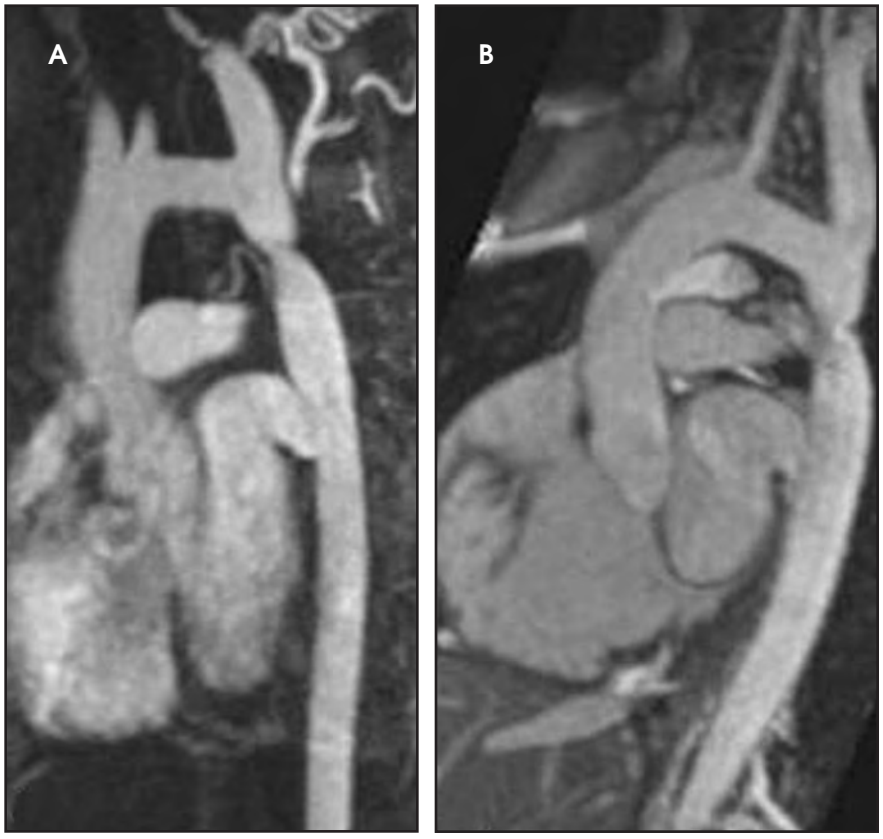

FIGURE 14. *Coarctation of the thoracic aorta as seen on (A) a 3-dimensional (3D) contrast-enhanced (CE) MR angiography (MRA) and (B) a 3D steady-state free-precession (SSFP) MRA. The relative merits of each technique are clearly evident, CE-MRA provides superior vascular delineation because of higher spatial resolution; while the respiratory and cardiac-gated SSFP-MRA is relatively free from motion artifact, so cardiac morphology is more clearly visualized.*

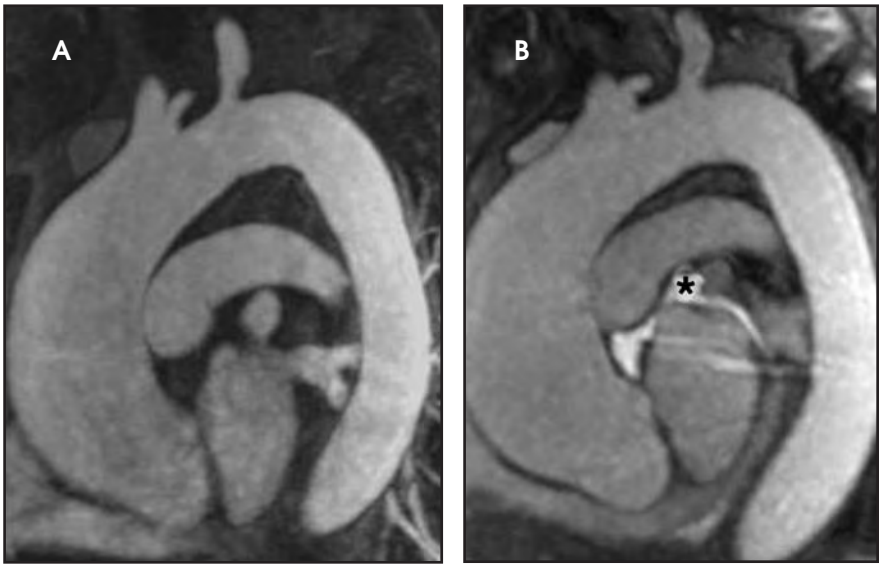

FIGURE 15. *A thoracic aortic aneurysm as seen on (A) a contrast-enhanced MR angiography (CE-MRA) and (B) a steady-state free-precession (SSFP) MRA. As in Figure 11, the freedom from cardiac motion allows improved delineation of the aortic root, as evidenced in this case of thoracic aortic aneurysm with superior visualization of the proximal thoracic aorta on (B) SSFP MRA, compared with (A) CE-MRA. Note, also the hyperintense signal of epicardial fat on the SSFP sequence (*).*

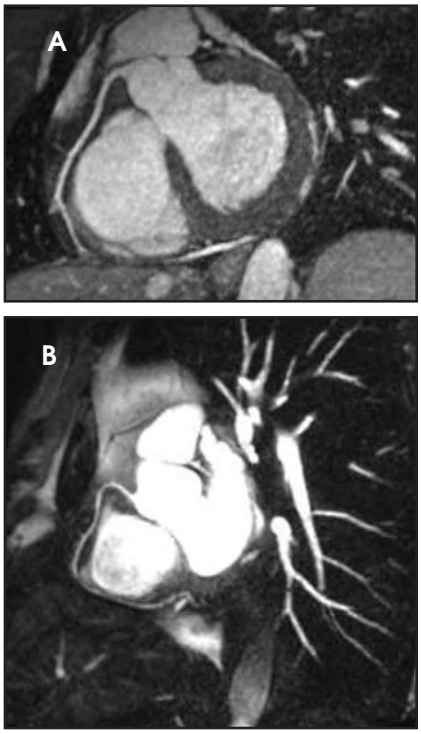

FIGURE 16. *Corresponding (A) free-breathing nonenhanced steady-state free-precession MR angiography (MRA) and (B) contrast-enhanced MRA of the right coronary artery in a normal subject.*

The development of parallel acquisition techniques[59,60] has provided a springboard for immense advances in the performance of CE-MRA applications. Concurrent technical advances in RF hardware have facilitated parallel data acquisition, which involves undersampling of k-space, and coil sensitivity profiles are used to calculate the missing k-space data.[61] Parallel acquisition invokes a penalty in SNR, a limitation that may be mitigated by imaging at higher field strengths such as 3T. As a result, high spatial resolution imaging over large fields of view during a fraction of the time required for full k-space sampling has become a routine tool, greatly advancing the clinical utility of CE-MRA. Indeed, the high sensitivity and specificity of this technique has been convincingly shown when imaging the carotid arteries, the renal arteries, and the thoracic and abdominal aorta in both children and adults.[62-64] Furthermore, the development of complex RF surface coil arrays with up to 32 receiver channels (or more) has resulted in high-performance MRA from the carotid arteries to the calf trifurcation vessels.[65]

A specific implementation of CE-MRA worthy of special mention is time-resolved MRA, during which a fast gradient-echo 3D sequence can clarify the temporal sequence of vascular and cardiac chamber enhancement.[66,67] Three-dimensional data sets can be acquired within 1 to 2 seconds and repeated for as long as required to image dynamic changes. The performance of 3D time-resolved MRA can be increased by the use of parallel acquisition and temporal data sharing. Time-resolved echo-shared angiographic technique (TREAT)[68] or time-resolved imaging of contrast kinetics (TRICKS) combining view sharing[69] and parallel imaging allows dynamic imaging at high spatial and temporal resolutions following the administration of contrast doses as low as 0.05 mmol/kg.[70] Such high temporal resolution allows confident separation of the arterial and venous phases of contrast enhancement and can provide information regarding directional flow and visceral perfusion as well as quantify curve parameters such as time-to-peak (TTP) signal intensity, maximal upslope of the curve (MUS), maximal signal intensity (MSI), and mean transit time (MTT).[70] Furthermore, when used at 3T, this technique provides both functional and anatomic information, allowing a reduction in the dose of Gd administered. The results of recent research offers promise for very high performance in time-resolved MRA using vastly undersampled projection reconstruction imaging.[71,72]

Clinical applications

The spatial resolution of modern CE-MRA continues to increase to such a degree that confident visualization of peripheral vessels measuring only 2 to 3 mm is now possible. As a result, CE-MRA has replaced CCA in many

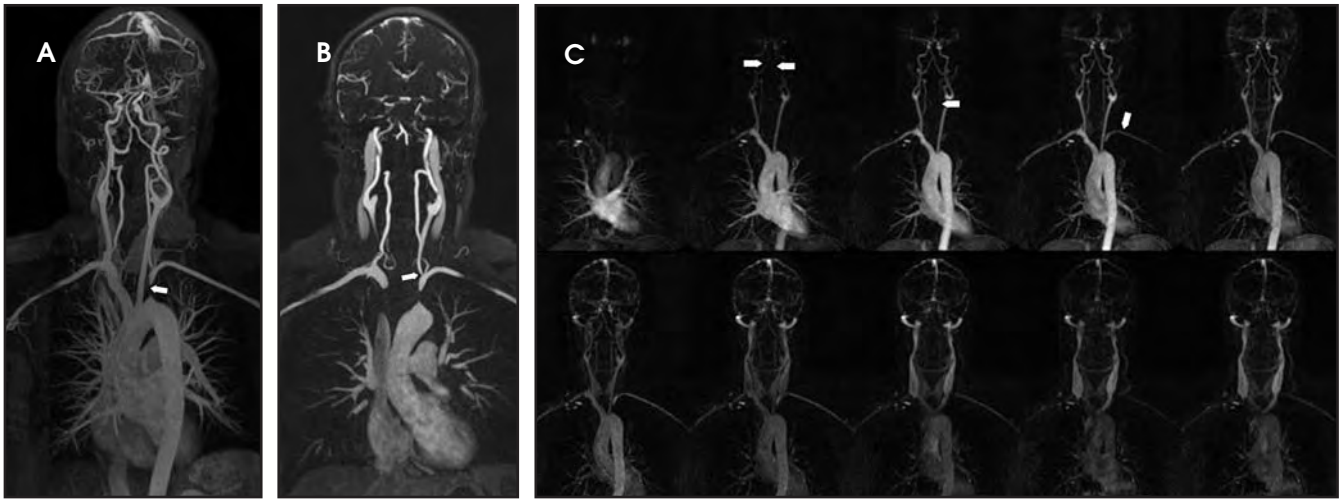

FIGURE 17. *Subclavian steal as seen on contrast-enhanced (CE) MR angiography (MRA) and time-resolved MRA examinations. (A) A full-thickness maximum-intensity projection (MIP) confirms the presence of a left subclavian near-occlusion. (B) This thin MIP CE-MRA reconstruction also illustrates the presence of a mild stenosis at the left vertebral arterial origin. Again, the direction of left vertebral flow may be only inferred from the data derived from CE-MRA. (C) Time-resolved MRA, however, shows both the sequence and temporal delay in supra-aortic vascular perfusion (arrows indicate source of perfusion of the left subclavian artery). Time-resolved MRA was performed with a 3 mL bolus of gadolinium.*

applications, allowing an alternative, less invasive, and clinically viable approach to vascular imaging. For this reason, CE-MRA has been successfully applied to every anatomic region, such that, in the absence of specific contraindications, its use should always be considered (Figures 17 through 19).

Established applications for CE-MRA include:

1) Atherosclerotic arterial occlusive disease that involves the carotid, abdominal aortic, renal, mesenteric, and peripheral extremity vessels;
2) Follow-up of the patency of surgically created vascular bypass grafts;
3) Assessment of pulmonary arterial patency in the presence of suspected acute or chronic pulmonary thromboembolic disease;
4) Exclusion of acute arterial insult, such as intramural hematoma, rupture, or dissection;
5) Diagnosis and follow-up of systemic vasculitis;
6) Investigation of the presence and extent of arteriovenous malformations, including distribution, soft tissue involvement, circulations involved, and degree of shunting.
7) Preoperative planning for a variety of surgical techniques, including donor assessment, considerations of thoracic and abdominal aortic aneurysms for endovascular repair, and evaluation of lower extremity vasculature prior to fibular free-flap creation; and
8) Diagnosis of central congenital vascular anomalies, including coarctation of the aorta and anomalous vessel origins and courses.

Discussion

Over the past several years, MRA has obviated the need for conventional catheter angiography in a variety of clinical situations. The advent of parallel imaging has helped to consolidate the role of CE-MRA as a practical diagnostic tool. Nonetheless, the versatility of nonenhanced techniques (including TOF-MRA for the intracranial circulation and 3D SSFP-MRA for much of the remaining vasculature) renders them viable alternatives to CE-MRA in patients in whom a contrast agent is contraindicated (eg, in pregnant patients), refused, or undesirable.

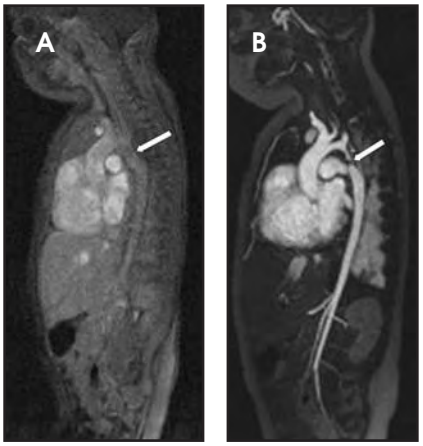

FIGURE 18. *A 4-month old infant with aortic coarctation, as seen on (A) an oblique sagittal FLASH and (B) a corresponding thin maximum-intensity projection contrast-enhanced MR angiographic (CE-MRA) reconstruction, performed after the administration of 2 mL of gadolinium contrast agent. Spin dephasing due to turbulence precludes visualization of the short-segment aortic interruption in A (arrow), in contrast to the high-resolution visualization achieved in B (arrow). Total contrast dosage for CE-MRA was 2 mL of gadolinium.*

Recent reports that link Gd administration to a rare disorder—nephrogenic systemic fibrosis—in patients with renal failure has generated concern about the use of CE-MRA in this patient population. Most cases to date have occurred in the context of dialysis-dependent patients who received high-dose Gd.[73,74] At the time of this writing, it is unclear what the ultimate implications of the association will be regarding the use of Gd contrast agents in this patient population. In the meantime, it would seem appropriate to minimize the dosage of Gd in susceptible patients. In instances in which the clinical indications for CE-MRA are strong, imaging at higher field strengths (such as 3T) permits reduction in the dosage of Gd contrast agent administered. Although much research remains to be done in this area, it may be that the requirement for dose reduction generates an additional impetus to perform CE-MRA at 3T, if available.

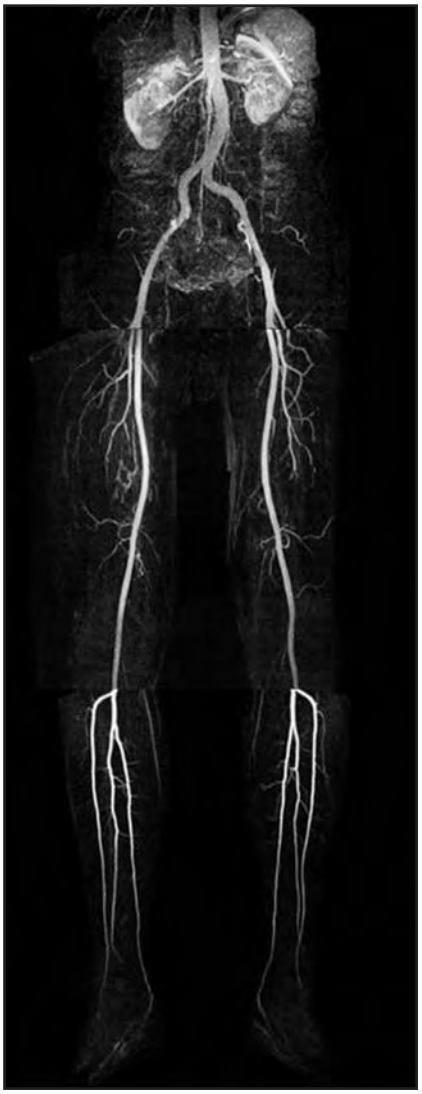

FIGURE 19. *Composite peripheral contrast-enhanced MR angiography performed on a 3T system. Note the high spatial resolution obtained over 3 large fields of view in the absence of detrimental venous contamination.*

As illustrated in Table 1, each MRA technique has specific strengths, clinical indications, and limitations, and, as a result, no single technique is optimal for all applications. Despite recent concerns regarding the use of Gd-based contrast in patients with severe renal impairment, these agents enjoy an impressive safety record, even compared with iodinated X-ray contrast agents.

As MR technology continues to evolve, newer and more powerful implementations of both contrast-enhanced and non–contrast-enhanced MRA will undoubtedly emerge.

Table 1. MRA techniques: Their advantages, disadvantages, and clinical applications.

MRA Technique	Advantages
2D TOF-MRA	Obviates the need for IV contrast administration. Highly sensitive to through-plane flow, more so than 3D TOF-MRA. Presaturation pulses enable definition of flow direction and generation of selective arteriograms or venograms. Relatively fewer saturation effects than with 3D TOF. May be used as a sequential breath-hold technique in the chest, abdomen, and pelvis. Useful for venous imaging.
3D TOF-MRA (including MOTSA)	Obviates the need for IV contrast administration. Allows isotropic high-resolution arbitrary voxel acquisition in nonmoving structures, if sufficient imaging time is allowed. Higher SNR. Larger anatomic coverage. Presaturation pulses enable definition of flow direction and generation of selective arteriograms or venograms.
2D PC-MRA	Sensitive to slow flow. Short acquisition times. Excellent intrinsic background signal suppression. Minimal saturation effects.
3D PC-MRA	Higher SNR than 2D PC-MRA. Higher spatial resolution than 2D PC-MRA. Sensitive to slow flow. Excellent intrinsic background signal suppression. Allows quantitative determination of flow direction and velocity.
3D SSFP-MRA	Flexible, allowing breath-holding or free-breathing data acquisition. EKG-gating can eliminate motion artifact for cardiac and aortic root imaging. High SNR due to inflow effects and exploitation of different T2/T1 ratios of different tissues. High CNR.
Time-resolved-MRA	High temporal resolution. Separation of arterial and venous phases, eliminating venous contamination. Allows visualization of complex flow patterns. Enhancement as an indirect measure of perfusion. Provides information regarding directional flow. Allows attenuation of contrast dose administered. Allows derivation of quantitative data (TTP, MUS, etc.). Automatic subtraction of mask images.
CE-MRA	Immune to saturation, intravascular signal being dependent upon contrast concentration, not flow. Very short TR possible, minimizing acquisition time. Very short TE possible, minimizing signal loss due to intravoxel dephasing. Rapid data acquisition, capturing first pass of contrast bolus, allowing breath-holding, minimizing motion artifact. Large-volume coverage. High spatial resolution and CNR. Freedom from flow directional restrictions. May be implemented as a time-resolved acquisition, mapping the sequence of vascular enhancement. Very suitable for performance enhancement by parallel acquisition.

MRA = magnetic resonance angiography; TOF = time-of-flight; IV = intravenous; MOTSA = multiple overlapping thin-slab acquisition; PC = phase contrast; SSFP = steady-state free precession; EKG = electrocardiagraphic; TR = repetition time; TE = echo time; SAR = specific absorption rate; AVM = arteriovenous malformation; AVF/Gs = arteriovenous fistulas/grafts.

Disadvantages	Clinical Applications
Limited through-plane resolution, particularly in breath-hold applications. Signal limited by adjacent short T1 tissue. Sensitive to in-plane saturation. Relatively long TR (to allow inflow) increases acquisition time. Relatively long TE (to allow gradient moment nulling) increases sensitivity to signal loss in regions of disturbed flow. Use of presaturation pulses may introduce artifacts and pseudo-occlusion in regions of flow reversal (eg, subclavian steal).	Circle of Willis and intracranial MRA. Intracranial venous imaging when Gd contrast agent is contraindicated. Previously, carotid imaging; though now less desirable due to better alternatives.
Sensitive to through-plane and in-plane saturation. Signal limited by adjacent short T1 tissue. Relatively long TR (to allow inflow) increases acquisition time. Relatively long TE (to allow gradient moment nulling) increases sensitivity to signal loss in regions of disturbed flow. Use of presaturation pulses may introduce artifacts and pseudo-occlusion in regions of flow reversal (eg, subclavian steal).	Circle of Willis and intracranial MRA. Intracranial venous imaging when Gd contrast agent is contraindicated. Previously, carotid imaging; though now less desirable due to better alternatives.
Unidirectional flow imaging. Projectional technique. Velocity aliasing. Intravoxel dephasing.	Rarely used for purely vascular imaging purposes in current practice. Major application is flow directional and velocity quantification.
Time-consuming. Velocity aliasing. Intravoxel dephasing.	Rarely used for purely vascular imaging purposes in current practice. Major application is flow directional and velocity quantification.
Free-breathing SSFP-MRA has long acquisition times. Spin dephasing. Off-resonance artifacts. Intense fat signal intensity.	Coronary MRA, thoracic and abdominal aortic MRA, carotid MRA, renal MRA, and peripheral MRA; and concurrent cardiac imaging.
Limited spatial resolution or SNR as a compromise for advanced temporal resolution. Limited through-plane resolution. Projectional technique precluding separation of overlapping structures. Requires suspension of motion (ie, patient cooperation). SAR limitations. Contrast adverse reactions.	Neurovascular MRA, thoracic MRA, abdominopelvic MRA, peripheral MRA. Detection and classification of stent graft endoleak. Assessment of graft patency. Determination of arteriovenous transit times in high flow states (eg, AVM, AVF/Gs). Assessment of complex congenital heart disease.
Inadequate contrast bolus timing may result in nondiagnostic studies. Electronic injector required. Requires high-performance hardware for best results. Venous contamination. K-space filling artifacts. Requires patient cooperation. Expensive.	Contrast adverse reactions. Whole-body MRA, neurovascular MRA, thoracic MRA, abdominopelvic MRA, peripheral MRA. Assessment of complex congenital heart disease. Detection of stent graft endoleak. Assessment of graft patency.

CE = contrast-enhanced; SNR = signal-to-noise ratio; CNR = contrast-to-noise ratio; Gd = gadolinium; TTP = time-to-peak; MUS = maximal upslope of the curve;

REFERENCES

1. Bosmans H, Marchal G, Lukito G, et al. Time-of-flight MR angiography of the brain: Comparison of acquisition techniques in healthy volunteers. *AJR Am J Roentgenol.* 1995;164:161-167.
2. Laub GA, Kaiser WA. MR angiography with gradient motion refocusing. *J Comput Assist Tomogr.* 1988;12: 377-382.
3. Korosec FR, Mistretta CA. MR angiography: Basic principles and theory. *Magn Reson Imaging Clin N Am.* 1998;6:223-256.
4. Edelman RR, Wentz KU, Mattle HP, et al. Intracerebral arteriovenous malformations: Evaluation with selective MR angiography and venography. *Radiology.* 1989;173:831-837.
5. Finn JP, Edelman RR, Jenkins RL, et al. Liver transplantation: MR angiography with surgical validation. *Radiology.* 1991;179:265-269.
6. Nael K, Villablanca JP, Saleh R, et al. Contrast-enhanced MR angiography at 3T in the evaluation of intracranial aneurysms: A comparison with time-of-flight MR angiography. *AJNR Am J Neuroradiol.* 2006; 27:2118-2121.
7. Prince MR, Grist TM, Debatin JF. *3D Contrast MR Angiography*, 3rd ed. New York, NY: Springer Verlag; 2003:5.
8. Thornton FJ, Du J, Suleiman SA, et al. High-resolution, time-resolved MRA provides superior definition of lower-extremity arterial segments compared to 2D time-of-flight imaging. *J Magn Reson Imaging.* 2006; 24:362-370.
9. Finn JP, Goldmann A, Edelman RR. Magnetic resonance angiography in the body. *Magn Reson Q.* 1992;8:1-22.
10. Edelman RR, Zhao B, Liu C, et al. MR angiography and dynamic flow evaluation of the portal venous system. *AJR Am J Roentgenol.* 1989;153:755-760. Comment in: *AJR Am J Roentgenol.* 1990;154:901-902.
11. Finn JP, Zisk JH, Edelman RR, et al. Central venous occlusion: MR angiography. *Radiology.* 1993; 187:245-251.
12. Rollins N, Booth T, Shapiro K. MR venography in children with complex craniosynostosis. *Pediatr Neurosurg.* 2000;32:308-315.
13. Roditi GH, Buff BL, Longmaid HE. MR venography of left renal vein anomalies. *Clin Radiol.* 1996; 51:861-864.
14. Catalano C, Pavone P, Laghi A, et al. Role of MR venography in the evaluation of deep venous thrombosis. *Acta Radiol.* 1997;38:907-912.
15. Scarabino T, Carriero A, Magarelli N, et al. MR angiography in carotid stenosis: A comparison of three techniques. *Eur J Radiol.* 1998;28:117-125.
16. Mitra D, Connolly D, Jenkins S, et al. Comparison of image quality, diagnostic confidence and interobserver variability in contrast enhanced MR angiography and 2D time of flight angiography in evaluation of carotid stenosis. *Br J Radiol.* 2006;79:201-207.
17. Blatter DD, Parker DL, Robison RO. Cerebral MR angiography with multiple overlapping thin slab acquisition. Part 1. Quantitative analysis of vessel visibility. *Radiology.* 1991;179:805-811.
18. Davis WL, Warnock SH, Harnsberger HR, et al. Intracranial MRA: Single volume vs. multiple thin slab 3D time-of-flight acquisition. *J Comput Assist Tomogr.* 1993;17:15-21.
19. Melhem ER, Poon EK, Weinreich EM, et al. Comparison of 2D- and 3DFT multiple overlapping thin-slab acquisition TOF MR angiography in carotid disease. *J Neuroimaging.* 1998;8:3-7.
20. Prince MR, Yucel EK, Kaufman JA, et al. Dynamic gadolinium-enhanced three-dimensional abdominal MR arteriography. *J Magn Reson Imaging.* 1993;3: 877-881.
21. Maki JH, Chenevert TL, Prince MR. Three-dimensional contrast-enhanced MR angiography. *Top Magn Reson Imaging.* 1996;8:322-344.
22. Sodickson DK, Manning WK. Simultaneous acquisition of spatial harmonics (SMASH): Fast imaging with radiofrequency coil arrays. *Magn Reson Med.* 1997;38:591-603.
23. Griswold MA, Jakob PM, Nittka M, et al. Partially parallel imaging with localized sensitivities (PILS). *Magn Reson Med.* 2000;44:602-609.
24. Pruessmann KP, Weiger M, Scheidegger MB, Boesiger P. SENSE: Sensitivity encoding for fast MRI. *Magn Reson Med.* 1999;42:952-962.
25. Nael K, Ruehm SG, Michaely HJ, et al. Multistation whole-body high-spatial-resolution MR angiography using a 32-channel MR system. *AJR Am J Roentgenol.* 2007;188:529-539.
26. Michaely HJ, Herrmann KA, Kramer H, et al. High-resolution renal MRA: Comparison of image quality and vessel depiction with different parallel imaging acceleration factors. *J Magn Reson Imaging.* 2006; 24:95-100.
27. Leiner T, de Vries M, Hoogeveen R, et al. Contrast-enhanced peripheral MR angiography at 3.0 Tesla: Initial experience with a whole-body scanner in healthy volunteers. *J Magn Reson Imaging.* 2003;17: 609-614.
28. Gibbs GF, Huston J 3rd, Bernstein MA, et al. 3.0-Tesla MR angiography of intracranial aneurysms: Comparison of time-of-flight and contrast-enhanced techniques. *J Magn Reson Imaging.* 2005;21:97-102.
29. Nael K, Michaely HJ, Villablanca P, et al. Time-resolved contrast enhanced magnetic resonance angiography of the head and neck at 3.0 tesla: Initial results. *Invest Radiol.* 2006;41:116-124.
30. Nael K, Michaely HJ, Lee M, et al. Dynamic pulmonary perfusion and flow quantification with MR imaging, 3.0T vs. 1.5T: Initial results. *J Magn Reson Imaging.* 2006;24:333-339.
31. Nael K, Fenchel M, Salamon N, et al. Three-dimensional cerebral contrast-enhanced magnetic resonance venography at 3.0 Tesla: Initial results using highly accelerated parallel acquisition. *Invest Radiol.* 2006;41:763-768.
32. Nael K, Villablanca JP, Pope WB, et al. Supra-aortic arteries: Contrast-enhanced MR angiography at 3.0 T–Highly accelerated parallel acquisition for improved spatial resolution over an extended field of view. *Radiology.* 2007;242:600-609.
33. Anderson CM, Saloner D, Lee RE, et al. Assessment of carotid artery stenosis by MR angiography: Comparison with X-ray angiography and color-coded Doppler ultrasound. *Am J Neuroradiol.* 1992;13:989-1000; discussion 1005-1008.
34. Wesbey GE, Bergan JJ, Moreland SI, et al. Cerebrovascular magnetic resonance angiography: A critical verification. *J Vasc Surg.* 1992;16:619-628; discussion 628-632.
35. Koelfen W, Wentz U, Freund M, Scheltze C. Magnetic resonance angiography in 140 neuropediatric patients. *Pediatr Neurol.* 1995;12:31-38.
36. Wilman AH, Huston J 3rd, Reiderer SJ. Three-dimensional magnetization-prepared time-of-flight MR angiography of the carotid and vertebral arteries. *Magn Reson Med.* 1997;37:252-259.
37. Rasanen HT, Manninen HI, Vanninen RL, et al. Mild carotid artery atherosclerosis: Assessment by 3-dimensional time-of-flight magnetic resonance angiography, with reference to intravascular ultrasound imaging and contrast angiography. *Stroke.* 1999; 30:827-833.
38. Wilcock DJ, Jaspan T, Wothington BS. Problems and pitfalls of 3-D TOF magnetic resonance angiography of the intracranial circulation. *Clin Radiol.* 1995; 50:526-532.
39. Carr JC, Ma J, Desphande V, et al. High-resolution breath-hold contrast-enhanced MR angiography of the entire carotid circulation. *Am J Roentgenol.* 2002;178:543-549.
40. Yang CW, Carr JC, Futterer SF, et al. Contrast-enhanced MR angiography of the carotid and vertebrobasilar circulations. *Am J Neuroradiol.* 2005; 26:2095-2101.
41. Dumoulin CL, Souza SP, Walker MF, Wagle W. Three-dimensional phase contrast MR angiography. *Magn Reson Med.* 1989;9:139-149.
42. Marks MP, Pelc MJ, Ross MR, Enzmann DR. Determination of cerebral blood flow with a phase-contrast cine MR imaging technique: Evaluation of normal subjects and patients with arteriovenous malformation. *Radiology.* 1992;182:467-476.
43. Prince MR. Renal MR angiography: A comprehensive approach. *J Magn Reson Imaging.* 1998;8: 511-516.
44. Goyen M, Heuser LJ. Improved peripheral MRA using multi-velocity-encoding phase contrast-enhanced MRA techniques. *Acta Radiol.* 2000;41: 139-141.
45. Waldman GJ, Pattynama PM, Chang PC, et al. Magnetic resonance angiography of dialysis access shunts: Initial results. *Magn Reson Imaging.* 1996;14:197-200.
46. Westenberg JJ, van der Geest RJ, Wasser MN, et al. Objective stenosis quantification from post-stenotic signal loss in phase-contrast magnetic resonance angiographic datasets of flow phantoms and renal arteries. *Magn Reson Imaging.*1998;16:249-260.
47. Carr JC, Simonetti O, Bundy J, et al. Cine MR angiography of the heart with segmented true fast imaging with steady-state precession. *Radiology.* 2001;219:828-834.
48. Pereles FS, McCarthy RM, Baskaran V, et al. Thoracic aortic dissection and aneurysm: Evaluation with nonenhanced true FISP MR angiography in less than 4 minutes. *Radiology.* 2002;223:270-274.
49. Deshpande VS, Shea SM, Laub G, et al. 3D magnetization-prepared true-FISP: A new technique for imaging coronary arteries. *Magn Reson Med.* 2001;46:494-502.
50. Bi X, Deshpande V, Carr JC, Li D. Coronary artery magnetic resonance angiography (MRA): A comparison between the whole-heart and volume-targeted methods using a T2-prepared SSFP sequence. *J Cardiovasc Magn Reson.* 2006;8:703-707.
51. Wansapura J, Fleck R, Crotty E, Gottliebson W. Frequency scouting for cardiac imaging with SSFP at 3 Tesla. *Pediatr Radiol.* 2006;36:1082-1085.
52. Greil GF, Desai MY, Fenchel M, et al. Reproducibility of free-breathing cardiovascular magnetic resonance coronary angiography. *J Cardiovasc Magn Reson.* 2007;9:49-56.
53. Miyazaki M, Sugiura S, Tateishi F, et al. Non-contrast-enhanced MR angiography using 3D ECG-synchronized half-Fourier fast spin echo. *J Magn Reson Imaging.* 2000;12:776-783.
54. Katoh M, Spuentrup E, Stuber M, et al. Free-breathing renal magnetic resonance angiography with steady-state free-precession and slab-selective spin inversion combined with radial k-space sampling and water-selective excitation. *Magn Reson Med.* 2005; 53:1228-1233.
55. Zavodni AE, Emery DJ, Wilman AH. Performance of steady-state free precession for imaging carotid

artery disease. *J Magn Reson Imaging*. 2005;21: 86-90.
56. Huegli RW, Aschwanden M, Scheffler K, Bilecen D. Fluoroscopic contrast-enhanced MR angiography with a magnetization-prepared steady-state free precession technique in peripheral arterial occlusive disease. *AJR Am J Roentgenol*. 2006;187:242-247.
57. Creasy JL, Price RR, Presbrey T, et al. Gadolinium-enhanced MR angiography. *Radiology*. 1990; 175:280-283.
58. Low G, Mizza A, Ong K, et al. Technical inadequacies of peripheral contrast-enhanced magnetic resonance angiography: Incidence, causes and management strategies. *Clin Radiol*. 2006;61: 937-945.
59. Niendorf T, Sodickson DK. Parallel imaging in cardiovascular MRI: Methods and applications. *NMR Biomed*. 2006;19:325-341.
60. Pruessmann KP. Parallel imaging at high field strength: Synergies and joint potential. *Top Magn Reson Imaging*. 2004;15:237-244.
61. Sodickson DK, McKenzie CA, Li W, et al. Contrast-enhanced 3D MR angiography with simultaneous acquisition of spatial harmonics: A pilot study. *Radiology*. 2000;217:284-289.
62. Clevert DA, Johnson T, Michaely H, et al. High-grade stenoses of the internal carotid artery: Comparison of high-resolution contrast enhanced 3D MRA, duplex sonography and power Doppler imaging. *Eur J Radiol*. 2006;60:379-386.
63. Michaely HJ, Herrmann KA, Kramer H, et al. High-resolution renal MRA: Comparison of image quality and vessel depiction with different parallel imaging acceleration factors. *J Magn Reson Imaging*. 2006; 24:95-100.
64. Chung T, Muthupillai R. Application of SENSE in clinical pediatric body MR imaging. *Top Magn Reson Imaging*. 2004;15:187-196.
65. Lin J, Chen B, Wang JH, et al. Whole-body three-dimensional contrast-enhanced magnetic resonance (MR) angiography with parallel imaging techniques on a multichannel MR system for the detection of various systemic arterial diseases. *Heart Vessels*. 2006;21: 395-398.
66. Finn JP, Baskaran V, Carr JC, et al. Thorax: Low-dose contrast-enhanced three-dimensional MR angiography with subsecond temporal resolution–Initial results. *Radiology*. 2002;224:896-904.
67. Carr JC, Laub G, Zheng J, et al. Time-resolved three-dimensional pulmonary MR angiography and perfusion imaging with ultrashort repetition time. *Acad Radiol*. 2002;9:1407-1418.
68. Fink C, Ley S, Kroeker R, et al. Time-resolved contrast-enhanced three-dimensional magnetic resonance angiography of the chest: Combination of parallel imaging with view sharing (TREAT). *Invest Radiol*. 2005;40:40-48.
69. Korosec FR, Frayne R, Grist TM, Mistretta CA. Time-resolved contrast-enhanced 3D MR angiography. *Magn Reson Med*. 1996;36:345-351.
70. Michaely HJ, Nael K, Schoenberg SO, et al. Renal perfusion: Comparison of saturation-recovery TurboFLASH measurements at 1.5T with saturation-recovery TurboFLASH and time-resolved echo-shared angiographic technique (TREAT) at 3.0T. *J Magn Reson Imaging*. 2006;24:1413-1419.
71. Du J, Lu A, Block WF, et al. Time-resolved undersampled projection reconstruction magnetic resonance imaging of the peripheral vessels using multi-echo acquisition. *Magn Reson Med*. 2005;53:730-734.
72. Mistretta CA, Wieben O, Velikina J, et al. Highly constrained backprojection for time-resolved MRI. *Magn Reson Med*. 2006;55:30-40.
73. Broome DR, Girguis MS, Baron PW, et al. Gadodiamide-associated nephrogenic systemic fibrosis: Why radiologists should be concerned. *AJR Am J Roentgenol*. 2007;188:586-592.
74. Chewning RH, Murphy KJ. Gadolinium-based contrast media and the development of nephrogenic systemic fibrosis in patients with renal insufficiency. *J Vasc Interv Radiol*. 2007;18:331-333.

CME Test Contrast-Enhanced MRA Versus Nonenhanced MRA, May 2007

To receive 2 CME credits, you must answer these test questions either online (follow the instructions on the inside front cover of this publication) or on the answer form on the opposite page (fax or mail it to Anderson Publishing).

1. Which of the following is correct regarding time-of-flight (TOF) imaging?
   A. Phase dispersion occurring in regions of turbulence has a tendency toward underestimation of the degree of stenoses.
   B. Multiple overlapping thin-slab acquisition (MOTSA) techniques are less susceptible to flow saturation effects than are single-slab 3-dimensional (3D) TOF magnetic resonance angiography (MRA) techniques.
   C. The administration of intravenous gadolinium contrast is more helpful for arterial than for venous imaging.
   D. Signal-to-noise ratio may be optimized by reduction of TR to the minimal value attainable.

2. Which of the following is a true statement regarding MRA?
   A. When imaging high-flow vascular systems, saturation effects are likely to affect 2-dimensional (2D) TOF-MRA to a greater degree than 3D TOF-MRA.
   B. MOTSA TOF-MRA offers the ability to perform volumetric data analysis in a fraction of the time allowable by 3D TOF-MRA.
   C. A review of the 3D TOF-MRA source data as well as of the reconstructed maximum intensity projection (MIP) images is recommended so that stenosis is not overestimated.
   D. Phase-contrast MRA is as dependent upon rapid inflow of unsaturated protons for signal generation as TOF-MRA.

3. When compared with 3D TOF-MRA, which of the following statements is true regarding phase-contrast MRA (PC-MRA)?
   A. It has a higher sensitivity to slow flow.
   B. It suffers to a greater extent from intravoxel dephasing.
   C. Flow signal is independent of blood velocity.
   D. It allows rapid 3D imaging.

4. Using current MRI systems, which of the following techniques has, on average, the smallest voxel dimensions?
   A. TOF-MRA
   B. PC-MRA
   C. Steady-state free-precession (SSFP) MRA
   D. Contrast-enhanced (CE) MRA

5. SSFP MRA has which of the following characteristics?
   A. Freedom from flow-related artifacts
   B. The ability to perform rapid, large field-of-view vascular imaging
   C. Compatibility with cardiac and respiratory gating
   D. High signal-to-noise ratio with limited contrast-to-noise ratio

6. Which of the following statements regarding contrast-enhanced MRA is false?
   A. Imaging at higher field strengths such as 3T allows a reduction in the dose of gadolinium administered.
   B. Submillimeter isotropic voxel acquisition is now possible over large fields of view.
   C. Spin dephasing in regions of complex flow limits its application to the intracranial circulation.
   D. Increasing the acceleration factor in parallel imaging results in a decrease in signal-to-noise ratio.

7. Which of these comments regarding the data acquisition during CE-MRA is accurate?
   A. Parallel imaging may be utilized to obtain increased coverage, temporal resolution, or spatial resolution during CE-MRA.
   B. Parallel imaging permits k-space filling by simultaneous signal sampling from multiple coil elements.
   C. Electrocardiographic-gating can minimize cardiac motion.
   D. To maintain image contrast uniformity, the center of k-space should be filled, as contrast is washing-out of the region in question.

8. Which of the following is true regarding time-resolved MRA?
   A. It involves multiple gadolinium injections over a defined period of time.
   B. It allows confident separation of arterial and venous phases for the majority of applications.
   C. It may be performed as a two-dimensional or three-dimensional technique.
   D. It does not have the ability to demonstrate directional blood flow.

9. Regarding intracranial vascular imaging, which of the following statements is true?
   A. TOF-MRA is superior to CE-MRA for both arterial and venous applications.
   B. Time-resolved MRA has little, if any, role to play in neurovascular imaging.
   C. Given its freedom from complex flow artifacts, SSFP-MRA is a valuable method for imaging the circle of Willis.
   D. Complete head-and-neck isolated arterial-phase imaging using CE-MRA has become a reality in recent times because of advances in parallel imaging.

10. Regarding the various nonenhanced and enhanced MRA techniques described, which of the following comments is false?
    A. For high-resolution vascular imaging of the chest and abdomen, gadolinium-enhanced techniques and non–gadolinium-enhanced techniques are equally practical.
    B. TR-MRA and high-resolution static CE-MRA represent complementary contrast-enhanced techniques, capable of providing high-spatial-resolution morphological and dynamic information.
    C. Contrast-enhanced MRA has superseded nonenhanced techniques in the majority of current clinical applications.
    D. Nonenhanced coronary artery imaging with SSFP-MRA can be used to evaluate for anomalous coronary anatomy.

Answer Form Contrast-Enhanced MRA Versus Nonenhanced MRA, May 2007

Use this form to fax or mail your answers to Anderson Pubishing. The test can also be completed online (see inside front cover).

Participant Information

Name	Title	Institution	
Street Address	City	State	ZIP
Email address	Telephone	License #	State of Licensure
I certify that I have studied the course materials and have personally completed the course test.		Date	

Signature

Test Answers (Please fill in the circle next to your answer)

1. ○A ○B ○C ○D

2. ○A ○B ○C ○D

3. ○A ○B ○C ○D

4. ○A ○B ○C ○D

5. ○A ○B ○C ○D

6. ○A ○B ○C ○D

7. ○A ○B ○C ○D

8. ○A ○B ○C ○D

9. ○A ○B ○C ○D

10. ○A ○B ○C ○D

Activity Evaluation (Please circle your rating for each item)

	Very satisfied	Satisfied	Undecided	Dissatisfied	Very dissatisfied
Content conducive to my learning	1	2	3	4	5
Manner and skill of presentation	1	2	3	4	5
Content relevant to my work	1	2	3	4	5
Content covered the published activity description	1	2	3	4	5
Content unbiased and nonpromotional	1	2	3	4	5
Overall, how satisfied were you?	1	2	3	4	5

Comments

☐ I would be interested in participating in future educational programs like this one.

You may fax this form to Anderson Pubishing at 908-301-1997 or mail it to Anderson Publishing,180 Glenside Avenue, Scotch Plains, NJ 07076. Your certificate will be sent to you by mail.

Supported by an educational grant from

GE Healthcare